*Pure Appl. Chem.*, Vol. 83, No. 8, pp. 1555–1565, 2011.
doi:10.1351/PAC-CON-11-02-05


# Enzymatic catalysis of proton transfer and decarboxylation reactions*

John P. Richard

*Department of Chemistry, University at Buffalo, Buffalo, NY 14260, USA*

*Abstract*: Deprotonation of carbon and decarboxylation at enzyme active sites proceed through the same carbanion intermediates as for the uncatalyzed reactions in water. The mechanism for the enzymatic reactions can be studied at the same level of detail as for nonenzymatic reactions, using the mechanistic tools developed by physical organic chemists. Triosephosphate isomerase (TIM)-catalyzed interconversion of D-glyceraldehyde 3-phosphate (GAP) and dihydroxyacetone phosphate (DHAP) is being studied as a prototype for enzyme-catalyzed proton transfer, and orotidine monophosphate decarboxylase (OMPDC)-catalyzed decarboxylation of orotidine 5'-monophosphate (OMP) is being studied as a prototype for enzyme-catalyzed decarboxylation. $^1$H NMR spectroscopy is an excellent analytical method to monitor proton transfer to and from carbon catalyzed by these enzymes in $D_2O$. Studies of these *partial* enzyme-catalyzed exchange reactions provide novel insight into the stability of carbanion reaction intermediates, which is not accessible in studies of the full enzymatic reaction. The importance of flexible enzyme loops and the contribution of interactions between these loops and the substrate phosphodianion to the enzymatic rate acceleration are discussed. The similarity in the interactions of OMPDC and TIM with the phosphodianion of bound substrate is emphasized.

*Keywords*: carbon acids; carbanions; enzyme catalysis; isotopes; kinetics; proton transfer; structure-reactivity.

## INTRODUCTION

Enzymes are extraordinarily powerful biological catalysts of otherwise slow reactions. They function to stabilize the high energy transition states of their reaction: Linus Pauling noted in 1948 that such large transition-state stabilization can be achieved through the development of very strong binding interactions between the protein and the transition state [1]. An understanding of the *mechanism* for enzymatic catalysis requires first of all a knowledge of the catalytic residues at the enzyme active site, of any reaction intermediates, and of the position of these residues relative to the enzyme-bound substrate and any bound intermediates. An examination of the X-ray crystal structure of the relevant protein–ligand complexes can often solve the problem of determining enzymatic reaction mechanisms at this level. The determination of the *mechanism* for stabilization of the enzyme-bound transition state is a much more difficult problem, because of the very short lifetime of $\approx 10^{-13}$ s for transition states. In principal, this problem might be solved by the application of the tools of mechanistic analysis developed by physical organic chemists over the past 75 years. Enzymologists, who are currently working to determine the mechanism by which protein catalysts stabilize their transition states, are adding to the toolbox of experimental protocol for the determination of complex reaction mechanisms.

*Paper based on a presentation made at the 20th International Conference on Physical Organic Chemistry (ICPOC-20), Busan, Korea, 22–27 August 2010. Other presentations are published in this issue, pp. 1499–1565.

## DECARBOXYLATION AND PROTON-TRANSFER REACTIONS

For the past 20 years, we have been interested in determining the rate and equilibrium constants for formation of carbanions stabilized by simple functionality such as an α-thioester [2], α-ester [3], α-nitrile [4], α-amide [5], and carbanions generated by deprotonation α-amino acids and α-amino carbon at peptides [6–8]. We have more recently become interested in determining the mechanism for formation of carbanions at enzyme active site, with a particular emphasis on understanding the mechanism by which enzymes achieve their large stabilization of the transition states for bond cleavage reactions that generate carbanions [9–11].

Two classes of organic reactions through carbanion intermediates are shown in Fig. 1. The top reaction is decarboxylation that proceeds by breakdown of a carboxylic acid with loss of $CO_2$ to form a carbanion, which is then protonated. The bottom reaction is isomerization that proceeds by loss of a proton from a carbon acid to form a carbanion, which undergoes unimolecular rearrangement followed by protonation to form product. These mechanisms share a carbanion intermediate, which undergoes protonation. They differ in the pathway for generation of the carbanion, which involves loss of $CO_2$ for decarboxylation and proton transfer for the isomerization reaction.

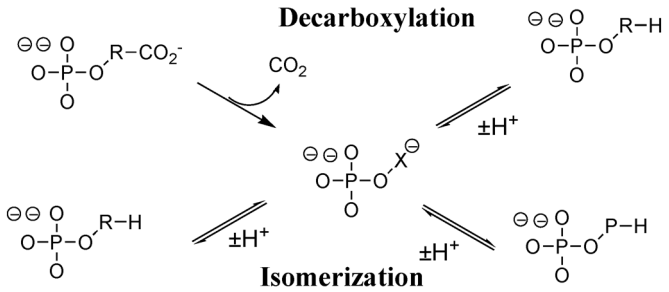


**Fig. 1** Examples of generic enzyme-catalyzed decarboxylation and isomerization reactions of substrates that contain a phosphodianion group to provide intrinsic binding energy for the stabilization of the transition state. The carbanion intermediate of the isomerization reaction undergoes rearrangement to covert substrate fragment R at product fragment P.

We are now studying the triosephosphate isomerase (TIM)-catalyzed interconversion of D-glyceraldehyde 3-phosphate (GAP) and dihydroxyacetone phosphate (DHAP) as a prototype for enzyme-catalyzed isomerization and the orotidine monophosphate decarboxylase (OMPDC)-catalyzed decarboxylation of orotidine 5'-monophosphate (OMP) to uridine 5'-monophosphate (UMP) as a prototype for enzyme-catalyzed decarboxylation (Fig. 2). TIM catalyzes a reaction on the remarkably successful glycolytic pathway, which was evident in the Archean period nearly 4 billion years ago [12]. The mechanism of action of TIM has attracted the attention of many enzymologists [13,14]. This is because proton transfer at carbon is a fundamental reaction in organic chemistry and cellular metabolic pathways, which is catalyzed by an incredibly broad range of enzymes. Lessons on the mechanism for enzyme-catalyzed proton transfer learned through studies on TIM, an enzyme with the classic TIM barrel protein fold [15,16] that appeared early in evolution, might therefore be generalized to enzymes *descended* from TIM. OMPDC is a remarkable enzyme because it employs no metal ions or other cofactors but yet effects an enormous ca. 30 kcal/mol stabilization of the transition state for the chemically very difficult decarboxylation of OMP to give uridine UMP [17]. The magnitude of these binding interactions is stunning, for the low-molecular-weight substrate OMP. We are interested in defining the relevant protein ligand interactions and in understanding the mechanism by which these interactions are specifically expressed at the transition state for the decarboxylation reaction.

 

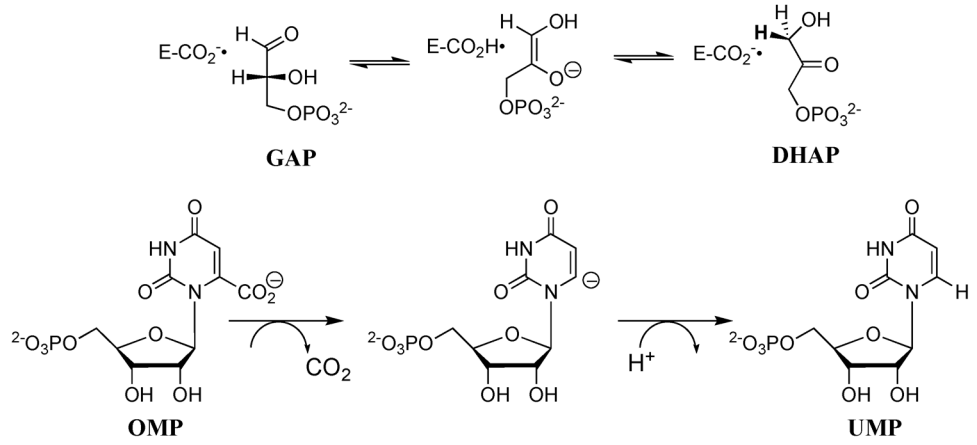


**Fig. 2** The isomerization reaction catalyzed by TIM, and the decarboxylation reaction catalyzed by orotidine 5'-phosphate decarboxylase.

## PROBES FOR ENZYME-CATALYZED PROTON-TRANSFER REACTIONS

### Triosephosphate isomerase

$^1$H NMR spectroscopy is a powerful analytical method for monitoring proton transfer from carbon in $D_2O$. It has been successfully used in determination of the carbon acidity of simple functional groups [2–8,18]. This technique provides very useful information about both the extent and the position of incorporation of deuterium into carbon acids. It is well suited for studies on the mechanism of action of TIM, because in $D_2O$ the enediol(ate) intermediate is known to partition between intramolecular transfer of the substrate hydrogen to product and exchange of this hydrogen with deuterium from solvent. The deuterium-labeled enzyme then partitions between reaction to form an aldehyde (GAP) and a ketone (DHAP) labeled with deuterium at the α-position. These reaction products are shown in Fig. 3 for the TIM-catalyzed reaction of GAP [19]. We have determined the yields of the products of the TIM-catalyzed reactions of GAP [20] and of DHAP [19] in $D_2O$. The results of these studies are in good qualitative agreement with the results of earlier studies by Knowles and co-workers using a tritium label in either the aqueous solvent or in the substrate DHAP [21]. However, our protocol is sim-

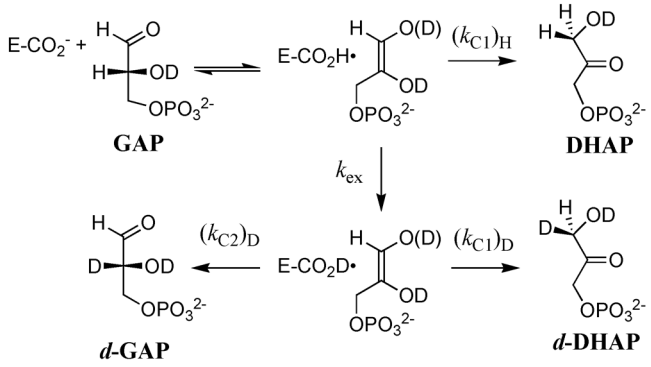


**Fig. 3** The three products of the TIM-catalyzed reaction of GAP in $D_2O$: DHAP from isomerization with intramolecular transfer of hydrogen, [1(*R*)-$^2$H]-DHAP from isomerization with incorporation of deuterium from $D_2O$ into C-1 of DHAP, and [2(*R*)-$^2$H]-GAP from incorporation of deuterium from $D_2O$ into C-2 of GAP [19].

 

pler and faster and provides a more complete set of product data than the analyses used in earlier studies of TIM employing tritium at tracer levels as the second hydrogen isotope [21]. They have resulted in several conclusions that have advanced our understanding of the dynamics of the proton-transfer reactions at the restricted confines of the enzyme active site [19,20,22].

(1) The TIM-catalyzed isomerization of GAP in $D_2O$ proceeds with 49 % intramolecular transfer of the $^1H$ label from substrate to product DHAP [19]. This stands in sharp contrast with the ≤6 % intramolecular transfer of the $^3H$ label from substrate to product GAP reported for the TIM-catalyzed reaction of [1(*R*)-$^3$H]-DHAP in $H_2O$ [23]. The data show that the hydron bound to the carboxylate side chain of Glu-165 in the TIM·enediol(ate) complex is *not* close to being in chemical equilibrium with the hydrons of bulk solvent.

(2) The ratios of the yields of the deuterium-labeled products *d*-DHAP and *d*-GAP from partitioning of the intermediate of the TIM-catalyzed reactions of GAP and DHAP in $D_2O$ are 1.48 and 0.93, respectively (Fig. 4). This provides evidence that the reaction of these two substrates does not proceed through a single, common, reaction intermediate, but rather through distinct intermediates that differ in the bonding and arrangement of catalytic residues at the enediolate O-1 and O-2 oxyanions formed on deprotonation of GAP and DHAP, respectively [20].

(3) The yield of hydrogen-labeled product DHAP from the TIM-catalyzed reaction of GAP in $D_2O$ remains constant as the concentration of the basic form of imidazole buffer is increased from 0.014 to 0.56 M. This shows that the active site of free-TIM, which has an open conformation needed to allow substrate binding, adopts a *closed* conformation at the enediolate-complex intermediate where the catalytic side chain of Glu-167 is *sequestered* from deprotonation by imidazole in the solvent $D_2O$ [22].

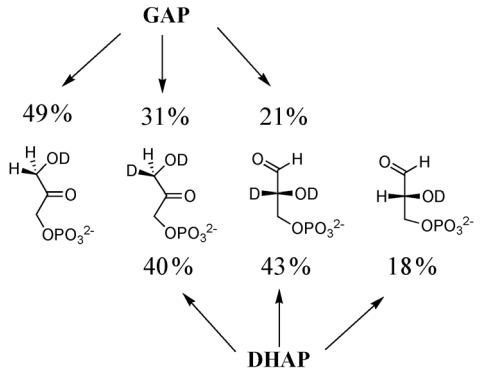


**Fig. 4** A comparison of the product yields for the TIM-catalyzed reactions of GAP and DHAP in $D_2O$.

## OMP DECARBOXYLASE

The very large kinetic barrier to the nonenzymatic decarboxylation of **OMP** ($t_{1/2}$ = 78 million years [17]) arises mainly from the thermodynamic barrier to formation of the highly unstable C-6 vinyl carbanion. This activation barrier may be reduced by interactions with OMPDC that either destabilize bound **OMP** relative to the bound carbanion intermediate, or by interactions that stabilize the bound carbanion intermediate relative to bound **OMP** [24]. OMPDC is assayed in the direction of decarboxylation of OMP, and mechanistic studies have naturally focused on the loss of $CO_2$ from substrate, which is the first stage in the stepwise reaction mechanism shown in Fig. 2. The second stage of proton transfer between the enzyme and substrate has received much less consideration in experimental and theoretical studies. This strong focus on the first reaction stage has resulted in a significant, but unappreci-

ated gap in our understanding of the enzymatic reaction mechanism, which can only be fully defined by studies that encompass the whole reaction.

The electrophilic substitution of $-CO_2$ by a proton may proceed by two reaction steps or stages: loss of $CO_2$ to form the putative vinyl carbanion reaction intermediate and protonation of this carbanion by an acidic catalytic residue to form UMP; or these two steps might be coupled in a concerted electrophilic substitution reaction. A product deuterium isotope effect (PIE) of 1.0 was determined as the ratio of the yields of [6-$^1$H]-uridine 5'-monophosphate (50 %) and [6-$^2$H]-uridine 5'-monophosphate (50 %) from the decarboxylation of OMP in 50/50 (v/v) HOH/DOD catalyzed by OMPDC from *S. cerevisiae*, *M. thermautotrophicus*, and *E. coli* [25,26]. This unitary PIE eliminates a proposed mechanism for enzyme-catalyzed decarboxylation in which proton transfer from Lys-93 to C-6 of OMP provides electrophilic *push* to the loss of $CO_2$ in a concerted reaction. The complete lack of selectivity for the reaction of solvent H and D has rarely been observed in chemical systems [27–29]. The result shows that the transferred hydron is a spectator at the rate-determining transition state. We have proposed that breakdown of OMP to form a C-6 UMP carbanion intermediate is the product-determining step. In this case, the product composition is already determined at the first step where substrate undergoes decarboxylation to form the vinyl carbanion intermediate, as explained in greater detail in the legend to Fig. 5.

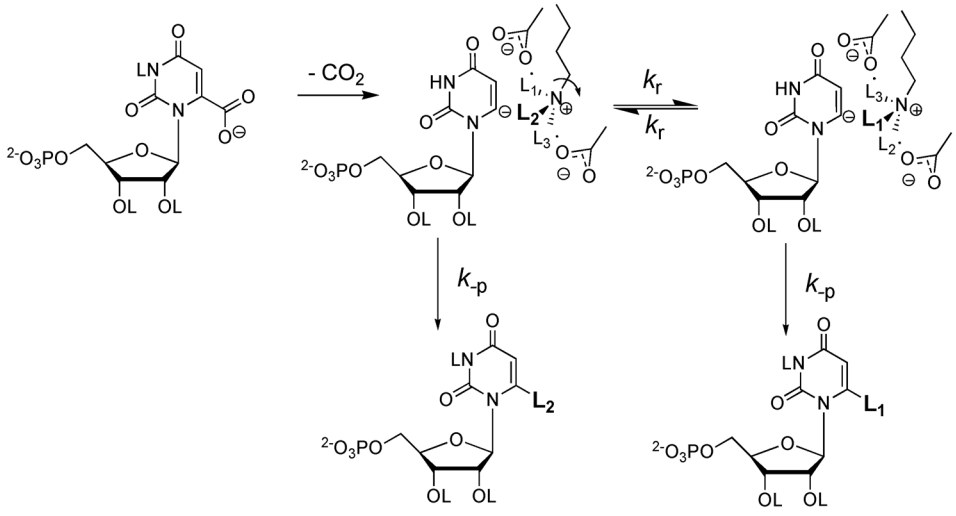


**Fig. 5** OMPDC-catalyzed decarboxylation in a mixed solvent of 50 % HOH ($L_1$) and 50 % DOD ($L_2$). There is no selectivity between the reaction of H and D, because the vinyl carbanion intermediate undergoes protonation by the hydron from the alkyl ammonium side chain of Lys-93 at a much faster rate than movement which exchanges the positions of the N-$L^+$ hydrons and allows the carbanion to select for reaction with H or D ($k_{-p} >> k_r$, Fig. 5). The product yield is determined by the fractionation factor $\Phi_{EL}$ for this acidic side chain. Values of $\Phi_{EL} \approx 1.0$ have been reported for H/D fractionation between $L_2O$ and R-$NL_3^+$ [30], so that the product isotope effect (PIE) of 1.0 is equal to the kinetic isotope effect (KIE).

We have considered the question of whether the catalytic rate acceleration for OMPDC is largely due to the stabilization of an enzyme-bound vinyl carbanion. A simple experiment to quantify the contribution of stabilization of a vinyl carbanion intermediate (Fig. 2) to the catalytic rate acceleration is to monitor formation of the carbanion as an intermediate of OMPDC-catalyzed exchange for deuterium of the C-6 proton of [6-$^1$H]-uridine 5'-monophosphate (***h*-UMP**) to give [6-$^2$H]-uridine 5'-monophosphate (***d*-UMP**, Fig. 6). We have used $^1$H NMR to show that OMPDC catalyzes exchange of the C-6 proton

of for deuterium from solvent in $D_2O$ at 25 °C and pD 7.0–9.3 (Fig. 6) [31]. Kinetic analysis of deuterium exchange gives $pK_a \leq 22$ for carbon deprotonation of enzyme-bound **UMP**, which is at least 10 units lower than that for deprotonation of an analog of **UMP** in water [32,33]. Our data show that yeast OMPDC stabilizes the bound vinyl carbanion by at least 14 kcal/mol [31]. There is a large increase in $k_{ex}$ ($s^{-1}$) with increasing pD and the leveling off at pD > 8. This shows that deuterium exchange is promoted by the basic form of an amino acid side chain at the active site of OMPDC. This catalytic base may be the neutral form of Lys-93, the catalytic side chain proposed to function to protonate the vinyl carbanion intermediate of the decarboxylation reaction (Fig. 6) [34]. We have also determined the kinetic parameters for OMPDC-catalyzed exchange for deuterium of the C-6 proton of 5-fluorouridine 5'-monophosphate where the electron-withdrawing 5-F provides a large stabilization of the carbanion-like reaction transition state for the deuterium exchange reaction [35].

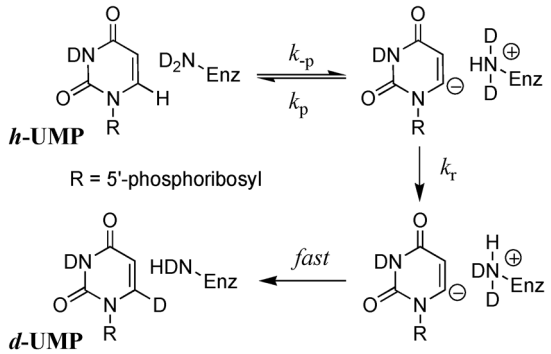


**Fig. 6** The mechanism for exchange for deuterium of the C-6 proton of ***h*-UMP** to give ***d*-UMP**.

## UTILIZATION OF PHOSPHODIANION BINDING ENERGY

One of the principal differences between enzymes and small molecule catalysts is that only enzymes have evolved mechanisms to utilize the binding interactions between the protein and nonreactive fragments of the substrate in the stabilization of the transition state at a site distant from this fragment [24]. This transmission of binding energy from a nonreactive binding determinant to a distant reaction center is a property unique to enzymatic catalysis. It has not been mimicked in the *de novo* design of protein catalysts, because the mechanism for this utilization of binding energy in transition-state stabilization is not understood.

The substrates for TIM and OMPDC bind at cavities on the protein surface, and each enzyme has a flexible loop which folds over the phosphodianion and sequesters their respective substrates from solvent. OMPDC has a second loop that interacts in a similar manner with the pyrimidine base of substrate. We have asked the following two questions about the contribution of the enzyme-phosphodianion binding interactions to the overall rate acceleration of these enzymes.

(1) *What is the total contribution of the enzyme-phosphodianion binding interactions to the rate acceleration for TIM and for OMPDC?* This contribution has been estimated by comparing the second-order rate constants for reaction of the whole substrate and for reaction of a truncated substrate that lacks the phosphodianion (Fig. 7). Truncation of the phosphodianion causes a $2 \times 10^9$ fold drop in the catalytic activity of TIM [36–38] and a $5 \times 10^8$ fold drop in the activity of OMPDC [39]. These effects correspond to an intrinsic phosphodianion binding energy of 12 kcal/mol, and a similar intrinsic phosphodianion binding energy has been determined for the reaction catalyzed by α-glycerol phosphate dehydrogenase [40,41]. It is interesting that there are two pathways for TIM-catalyzed deprotonation of GA. One pathway involves a reaction at the enzyme active site. There is a second nonspecific pathway.

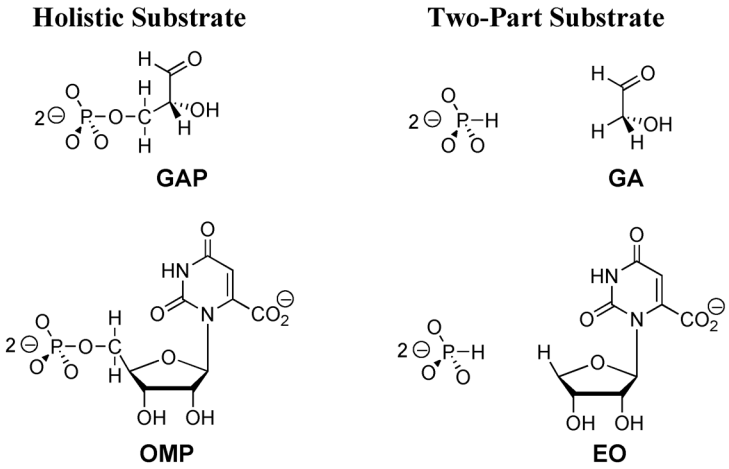


**Fig. 7** A comparison of the whole substrates with the corresponding pieces for the reactions catalyzed by TIM and OMPDC.

We find that TIM and bovine serum albumin (BSA) exhibit similar modest catalytic activity towards deprotonation of α-hydroxy α-carbonyl carbon by this nonspecific reaction pathway [42]. In other words, essentially the entire difference between the catalytic activity of TIM and BSA towards deprotonation of α-hydroxy α-carbonyl carbon is caused by the 12 kcal/mol intrinsic phosphodianion binding energy.

(2) *Are the protein phosphodianion interactions utilized mainly to anchor the substrate to the enzyme, or do they play the additional role of activating the enzyme for catalysis of the reaction of the bound substrate?* The demonstration that the interactions between the enzyme and the phosphodianion group are "catalytic" in the absence of a covalent connection to a truncated substrate analog provides unequivocal evidence that the oxydianion is not simply play the role of an "anchor". We have shown that addition of 1.0 M phosphite dianion causes a 50 000-fold increase in $k_{cat}/K_m$ for TIM-catalyzed turnover of the truncated substrate glycolaldehyde (GA), and a 600 000-fold increase in $k_{cat}/K_m$ for OMPDC-catalyzed turnover of the truncated substrate 1-(β-D-erythrofuranosyl)orotic acid (**EO**, Fig. 7) [39].

There is a large entropic advantage to the binding of the whole substrate compared to the truncated substrate piece and phosphite dianion [43], but the chemical reactivity of the enzyme-bound substrate pieces in their catalyzed reactions is similar to that for the enzyme-bound whole substrate. In fact, the value of $k_{cat}$ for turnover of **EO** and phosphite to give the product of decarboxylation was estimated to be greater than $k_{cat}$ for decarboxylation of **OMP** [39]. $^1$H NMR analysis shows that three products form from the phosphite-activated TIM-catalyzed reactions of [1-$^{13}$C]-GA in $D_2O$: [2-$^{13}$C]-GA from intramolecular transfer of the substrate-derived hydrogen to the $^{13}$C-labeled carbon of the enediolate reaction intermediate; (b) [1-$^{13}$C, 2-$^2$H]-GA from transfer of deuterium from solvent to the $^{12}$C-labeled carbon of the enediolate; and (c) [2-$^{13}$C, 2-$^2$H]-GA from transfer of deuterium from solvent to the $^{13}$C-labeled carbon of the enediolate [44]. In other words, TIM catalyzes an *isomerization* reaction of [1-$^{13}$C]-GA to [2-$^{13}$C]-GA. The yields of the products of these TIM-catalyzed reactions are similar to the yields of the corresponding products that form from the reaction of the whole substrate GAP in $D_2O$ (Fig. 3) [19,44].

The 19 residue phosphate gripper loop of the mesophilic ScOMPDC is much larger than the 9 residue loop at the ortholog from the thermophile *Methanothermobacter thermautotrophicus* (MtOMPDC). This difference in loop size results in only a small decrease in the total intrinsic phosphate binding energy of the phosphodianion group of OMP from 11.9 to 11.6 kcal/mol, along with a

modest decrease in the extent of activation by phosphite dianion of decarboxylation of the truncated substrate **EO** [45]. The activation parameters $\Delta H^{\ddagger}$ and $\Delta S^{\ddagger}$ for $k_{cat}$ for decarboxylation of OMP are 3.6 kcal/mol and 10 cal/K/mol more positive, respectively, for MtOMPDC than for ScOMPDC. These differences correlate with the difference in size of the active site loops at the mesophilic ScOMPDC and the thermophilic MtOMPDC. We have suggested that the greater enthalpic transition-state stabilization available from the more extensive loop-substrate interactions for the ScOMPDC-catalyzed reaction is largely balanced by a larger entropic requirement for immobilization of the larger loop at this enzyme [45].

The substrate phosphodianion, and the substrate piece phosphite dianion interact strongly with catalytic side chains at a flexible phosphate gripper loop and these interactions drive loop closure over the dianions and result in a large stabilization of carbanion-like transition states for the decarboxylation and deuterium exchange reactions, which is manifested as the high specificity in transition-state binding. The results may be rationalized using Fig. 8, where the enzyme exists mainly in the inactive open form ($\mathbf{E_O}$). The rare unliganded closed enzyme ($\mathbf{E_C}$) and the $HPO_3^{2-}$-liganded enzyme ($\mathbf{E_C}\cdot HPO_3^{2-}$) exhibit similar high reactivity in carbon deprotonation or decarboxylation of the appropriate truncated substrate, so that $k_{cat}/K_m = (k_{cat}/K_m)'$. The intrinsic binding energy of $HPO_3^{2-}$ is then utilized to drive the unfavorable conformational change from $\mathbf{E_O}$ to $\mathbf{E_C}$ [44]. If this model is correct, then the most important remaining challenge to understanding the mechanism of action of TIM and OMPDC is to provide a physical explanation for the proposed large effect of loop closure on the enzymatic activity towards catalysis of the reaction of the truncated substrate.

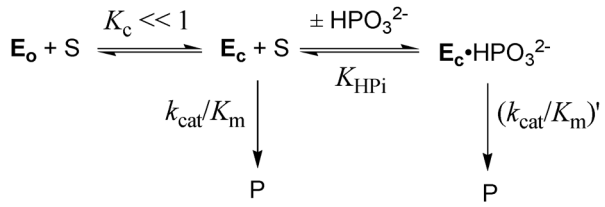


**Fig. 8** Model which shows the utilization of phosphite binding energy to stabilize $\mathbf{E_C}$, a rare form of TIM or OMPDC that shows a high activity for catalysis of the reaction of the truncated substrates **GA** or **EO**, respectively.

## CRITICAL INTERACTION BETWEEN A CATIONIC SIDE CHAIN AND THE SUBSTRATE PHOSPHODIANION

The ammonium ion side chain of Lys12 forms an ion pair with the phosphodianion group of DHAP or DGAP bound to TIM [46–48]. Similarly, there is good evidence that the guanidinium cation side chain of Arg-235 forms an ion pair with the phosphodianion group of OMP bound to OMPDC [34]. There is evidently little change in the position of these residues relative to the phosphodianion of bound DHAP or OMP as the flexible loop of TIM or OMPDC closes over the phosphodianion. The R235A mutation at yeast OMPDC results in a 1300-fold increase in $K_m$ and a 14-fold decrease in $k_{cat}$ for decarboxylation of OMP, corresponding to a 5.8 kcal/mol destabilization of the transition state for the decarboxylation reaction [49]. By comparison, the K12G mutation of TIM results in a 50-fold increase in $K_m$ and a 12 000-fold decrease in $k_{cat}$ for isomerization of GAP, corresponding to an even larger 7.8 kcal/mol destabilization of the transition state for isomerization [47]. We have proposed that the extremely large effect of the K12G mutation on the stability of the transition state for the TIM-catalyzed reaction is due to stabilizing electrostatic interactions between the cationic enzyme side chain and *both* the substrate phosphodianion and the negative charge that develops at the enolate-like oxygen in the transition state for deprotonation of GAP [47].

 

The activity of the K12G TIM mutant can be successfully "rescued" by $NH_4^+$ and primary alkylammonium cations. The transition state for the K12G mutant TIM-catalyzed reaction is stabilized by 1.5 kcal/mol by interaction with $NH_4^+$ [46]. The larger 3.9 kcal/mol stabilization by $CH_3CH_2CH_2CH_2NH_3^+$ is due to hydrophobic interactions between the mutant enzyme and the butyl side chain of the cation activator. A comparison of $k_{cat}/K_m = 6.6 \times 10^6$ $M^{-1}$ $s^{-1}$ for the wild-type TIM-catalyzed isomerization of GAP and the third-order rate constant of 150 $M^{-2}$ $s^{-1}$ for activation by $NH_4^+$ of the K12G mutant TIM-catalyzed isomerization shows that stabilization of the bound transition state by the effectively intramolecular interaction of the cationic side chain of Lys-12 at wild-type TIM is 6.3 kcal/mol greater than for the corresponding intermolecular interaction of $NH_4^+$ at K12G mutant TIM. These data are consistent with a ca. 6.3 kcal/mol entropic advantage of the effectively intramolecular interaction of the side chain of Lys-12 at wild-type TIM over the intermolecular interaction of an ammonium cation activator and the K12G mutant (Fig. 9).

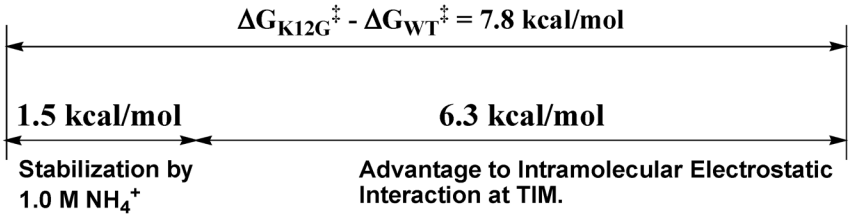


**Fig. 9** A comparison of the binding energy of primary ammonium cations to the transition state for K12G mutant TIM-catalyzed isomerization of GAP (1.5 kcal/mol) and the apparent transition-state stabilization obtained from connecting these activators to the mutant enzyme (6.3 kcal/mol). The sum of these terms is equal to the overall stabilization of the transition state for the wild-type TIM-catalyzed isomerization of GAP by interaction with the cationic side chain of Lys-12 (7.8 kcal/mol) [47].

We have also observed rescue of the R235A mutant of OMPDC by added guanidinium cation. There is a larger stabilization of the transition state for R235A mutant OMPDC by 1 M guanidinium cation (–2.8 kcal/mol) compared with the 1.5 kcal/mol activation of K12G mutant TIM by 1 M $NH_4^+$ despite the smaller stabilizing interaction of the guanidinium cation side chain of Arg-235 at OMPDC (5.8 kcal/mol effect of the R235A mutation) than of the alkylammonium cation side chain of Lys-12 at TIM (7.8 kcal/mol effect of the K12G mutation). We have not yet fully rationalized these quantitative differences in the rescue of these two mutant enzymes.

## CONCLUDING REMARKS

Our results have shown that appending a phosphodianion to organic substrates provides specificity in the binding of both the ground state and the transition state for enzyme-catalyzed proton transfer, hydride transfer, and decarboxylation reactions. They suggest that it is important to focus on the interactions between the enzyme and the whole substrate when trying to formulate a mechanism for stabilization of the transition state for the enzyme-catalyzed reaction of a reactive substrate piece. For example, interactions between protein catalysts and the coenzyme A fragment of acetyl CoA may provide critical stabilization of the transition state for formation of the thioester carbanion intermediates of enzyme-catalyzed Claisen condensation reactions.

 

## ACKNOWLEDGMENTS

We acknowledge the National Institutes of Health Grant GM39754 for generous support of the work presented in this lecture. The studies on OMP decarboxylase were part of a stimulating and fruitful collaboration with Prof. John Gerlt from the University of Illinois.

## REFERENCES

1. L. Pauling. *Nature* **161**, 707 (1948).
2. T. L. Amyes, J. P. Richard. *J. Am. Chem. Soc.* **114**, 10297 (1992).
3. T. L. Amyes, J. P. Richard. *J. Am. Chem. Soc.* **118**, 3129 (1996).
4. J. P. Richard, G. Williams, J. Gao. *J. Am. Chem. Soc.* **121**, 715 (1999).
5. J. P. Richard, G. Williams, A. C. O'Donoghue, T. L. Amyes. *J. Am. Chem. Soc.* **124**, 2957 (2002).
6. A. Rios, T. L. Amyes, J. P. Richard. *J. Am. Chem. Soc.* **122**, 9373 (2000).
7. A. Rios, J. P. Richard. *J. Am. Chem. Soc.* **119**, 8375 (1997).
8. A. Rios, J. P. Richard, T. L. Amyes. *J. Am. Chem. Soc.* **124**, 8251 (2002).
9. J. P. Richard, T. L. Amyes. *Curr. Op. Chem. Biol.* **5**, 626 (2001).
10. J. P. Richard, T. L. Amyes. *Bioorg. Chem.* **32**, 354 (2004).
11. T. L. Amyes, J. P. Richard. In *Hydrogen-Transfer Reactions, Vol. 3, Biological Aspects I-II*, J. T. Hynes, J. P. Klinman, H.-H. Limbach, R. L. Schowen (Eds.), pp. 949–973, Wiley-VCH, Weinheim (2007).
12. K. A. Webster. *J. Exp. Biol.* **206**, 2911 (2003).
13. J. R. Knowles. *Philos. Trans. R. Soc. London, Ser. B* **332**, 115 (1991).
14. I. A. Rose. *Brookhaven Symp. Biol.* **15**, 293 (1962).
15. N. Nagano, C. A. Orengo, J. M. Thornton. *J. Mol. Biol.* **321**, 741 (2002).
16. R. Sterner, B. Hocker. *Chem. Rev.* **105**, 4038 (2005).
17. A. Radzicka, R. Wolfenden. *Science* **267**, 90 (1995).
18. J. P. Richard, T. L. Amyes, M. M. Toteva. *Acc. Chem. Res.* **34**, 981 (2001).
19. A. C. O'Donoghue, T. L. Amyes, J. P. Richard. *Biochemistry* **44**, 2610 (2005).
20. A. C. O'Donoghue, T. L. Amyes, J. P. Richard. *Biochemistry* **44**, 2622 (2005).
21. J. R. Knowles, W. J. Albery. *Acc. Chem. Res.* **10**, 105 (1977).
22. A. C. O'Donoghue, T. L. Amyes, J. P. Richard. *Org. Biomol. Chem.* **6**, 391 (2008).
23. J. M. Herlihy, S. G. Maister, W. J. Albery, J. R. Knowles. *Biochemistry* **15**, 5601 (1976).
24. W. P. Jencks. *Adv. Enzymol. Relat. Areas Mol. Biol.* **43**, 219 (1975).
25. K. Toth, T. L. Amyes, B. M. Wood, K. Chan, J. A. Gerlt, J. P. Richard. *J. Am. Chem. Soc.* **132**, 7018 (2010).
26. K. Toth, T. L. Amyes, B. M. Wood, K. Chan, J. A. Gerlt, J. P. Richard. *J. Am. Chem. Soc.* **129**, 12946 (2007).
27. K.-Y. Wong, J. P. Richard, J. Gao. *J. Am. Chem. Soc.* **131**, 13963 (2009).
28. W.-Y. Tsang, J. P. Richard. *J. Am. Chem. Soc.* **129**, 10330 (2007).
29. W.-Y. Tsang, J. P. Richard. *J. Am. Chem. Soc.* **131**, 13952 (2009).
30. R. M. Jarret, M. Saunders. *J. Am. Chem. Soc.* **108**, 7549 (1986).
31. T. L. Amyes, B. M. Wood, K. Chan, J. A. Gerlt, J. P. Richard. *J. Am. Chem. Soc.* **130**, 1574 (2008).
32. A. Sievers, R. Wolfenden. *J. Am. Chem. Soc.* **124**, 13986 (2002).
33. F. Y. Yeoh, R. R. Cuasito, C. C. Capule, F. M. Wong, W. Wu. *Bioorg. Chem.* **35**, 338 (2007).
34. B. G. Miller, A. M. Hassell, R. Wolfenden, M. V. Milburn, S. A. Short. *Proc. Natl. Acad. Sci. USA* **97**, 2011 (2000).
35. K. K. Chan, B. M. Wood, A. A. Fedorov, E. V. Fedorov, H. J. Imker, T. L. Amyes, J. P. Richard, S. C. Almo, J. A. Gerlt. *Biochemistry* **48**, 5518 (2009).

 

36. T. L. Amyes, A. C. O'Donoghue, J. P. Richard. *J. Am. Chem. Soc.* **123**, 11325 (2001).
37. T. L. Amyes, J. P. Richard. *Biochemistry* **46**, 5841 (2007).
38. J. P. Richard. *J. Am. Chem. Soc.* **106**, 4926 (1984).
39. T. L. Amyes, J. P. Richard, J. J. Tait. *J. Am. Chem. Soc.* **127**, 15708 (2005).
40. W.-Y. Tsang, T. L. Amyes, J. P. Richard. *Biochemistry* **47**, 4575 (2008).
41. J. R. Morrow, T. L. Amyes, J. P. Richard. *Acc. Chem. Res.* **41**, 539 (2008).
42. M. K. Go, M. M. Malabanan, T. L. Amyes, J. P. Richard. *Biochemistry* **49**, 7704 (2010).
43. W. P. Jencks. *Proc. Natl. Acad. Sci. USA* **78**, 4046 (1981).
44. M. K. Go, T. L. Amyes, J. P. Richard. *Biochemistry* **48**, 5769 (2009).
45. K. Toth, T. L. Amyes, B. M. Wood, K. K. Chan, J. A. Gerlt, J. P. Richard. *Biochemistry* **48**, 8006 (2009).
46. M. K. Go, T. L. Amyes, J. P. Richard. *J. Am. Chem. Soc.* **132**, 13525 (2010).
47. M. K. Go, A. Koudelka, T. L. Amyes, J. P. Richard. *Biochemistry* **49**, 5377 (2010).
48. D. Joseph-McCarthy, E. Lolis, E. A. Komives, G. A. Petsko. *Biochemistry* **33**, 2815 (1994).
49. S. A. Barnett, T. L. Amyes, B. McKay Wood, J. A. Gerlt, J. P. Richard. *Biochemistry* **49**, 824 (2010).

 